Dynamics of fibroblast spreading

Graham A. Dunn* and Daniel Zicha

MRC Muscle and Cell Motility Unit, The Randall Institute, King's College London, 26-29 Drury Lane, London WC2B 5RL, UK

*Author for correspondence

SUMMARY

A new technique of microinterferometry permits cellular growth and motile dynamics to be studied simultaneously in living cells. In isolated chick heart fibroblasts, we have found that the non-aqueous mass of each cell tends to increase steadily, with minor fluctuations, throughout the cell cycle. The spread area of each cell also tends to increase during interphase but fluctuates between wide limits. These limits are dependent on the cell's mass and the upper limit is particularly sharp and directly proportional to mass. From a dynamical point of view, the spread area of a cell is determined by the balance between the rates of two antagonistic processes: protrusion of cellular material into new territory and retraction of material from previously occupied territory. The spatial asymmetry of these processes determines the translocation of the cell. We have found with the chick fibroblasts that the rates of the two processes are generally closely matched to each other and appear to be dependent on the cell's area of spreading. Both continue incessantly in well spread cells, even when there is no net translocation of the cell, and the lower limit

of each activity is directly proportional to spread area. The two processes show different behaviour, however, during changes in the spread area of the cell. Both increases and decreases in area appear to be brought about by changes in the rate of retraction, the rate of protrusion remaining relatively constant. A simple stochastic model based on a limited supply of adhesion molecules can simulate all our observations including the mass-limited spreading, the strong correlation between protrusion and retraction and the retraction-dominated changes in area. We conclude that the spread area of the cell is actively regulated, possibly by a simple automatic mechanism that adjusts the area of spreading in relation to the mass of the cell and controls the rate of protrusion to compensate rapidly for spontaneous fluctuations in retraction.

Key words: chick heart fibroblast, cell spreading, cell protrusion, cell retraction, cell adhesion, cell motility, cell growth, Horn interference microscopy, phase-shifting interferometry, phase-stepping interferometry, dry mass measurement

INTRODUCTION

In a pioneering paper on the motile dynamics of cultured heart fibroblasts, Weiss and Garber (1952), commenting on the use of visual criteria to describe cells, pronounced that, 'It is the task of contemporary biology to replace such static and purely formal descriptions of living systems by dynamic concepts which will define these systems objectively by reference to their inherent properties expressed in measurable standard units, rather than in terms of subjective impressions.' As part of a programme for developing such objective criteria for studying cell behaviour, we have introduced a new technique of microinterferometry which permits cell growth and the bulk movements of non-aqueous cellular material to be studied quantitatively in individual cells. Different cellular materials have very similar specific refraction increments and thus the retardation of a beam of light passing through a living cell is accurately proportional to the mass of non-aqueous material within the beam (Davies and Wilkins, 1952; Bereiter-Hahn, 1985; Brown and Dunn, 1989). By applying the technique of phase-stepping to transmission interference microscopy, we are now able to compute this retardation with sufficient accuracy, range and stability to study the growth and motility

of cultured cells over periods of hours or even days (Dunn and Zicha, 1993; Dunn and Zicha, 1994). The resulting images are digital maps of the dry mass distributions within the cells and long sequences of these images, recorded on hard disk at time-lapse rates, constitute a database which may be analysed in many different ways in order to study growth and motility.

In this paper we analyse a database of six phase-stepped image sequences of primary cultured chick heart fibroblasts - a total of 4320 images. The analysis concentrates on the relationship between mass distribution and spread area of the cells. An early hint that the spreading of heart fibroblasts may be actively controlled was reported by Weiss and Garber (1952), who stated that projections of the cell margin are in competitive interaction with one another such that the protrusion of one tends to be accompanied by the retraction of another. Such a relationship would obviously tend to maintain a constant spread area despite rapid changes in shape of the cell. Weiss and Garber proposed the explanation that a viscous flow of protoplasm into a protrusion exerts a draining suction on its surroundings in proportion to its momentum, and thus inhibits other protrusions in the vicinity, but we know from modern hydrodynamics that momentum is virtually irrelevant on the cellular scale (in which the Reynold's number - a hydro-

dynamic scaling factor - is very low). In any case, evidence has emerged that the cause/effect relationship between protrusion and retraction can be the other way round: that retraction can cause protrusion. Chen (1979) and Dunn and Heath (reported by Dunn, 1980) independently discovered that a wave of increased spreading activity follows about 20 seconds after retraction of the tail of a chick heart fibroblast. Chen called this phenomenon 'retraction-induced spreading' and it occurs whether the retraction is spontaneous or is brought about by detaching the tail from the substratum using a microneedle. Brown and Dunn (1989) used interference microscopy (without phase-stepping) and time-lapse intervals of 4 seconds to observe the rapid changes in mass distribution that follow spontaneous tail retractions. Using finite element analysis to obtain maps of the minimal rate of mass flow needed to account for the changes in mass distribution, they found that bulk flow velocities could be as high as almost 2 μm s^{-1} into regions of protrusion. The kinetic energy of this minimal mass flow, averaged over the whole cell, is a measure of intracellular motility and, after a large peak of kinetic energy associated with the tail retraction, a second peak associated with increased protrusive activity occurs 40-50 seconds later (unpublished analysis of the data obtained by Brown and Dunn).

The derivation of kinetic energy from interference images using finite element analysis is very computer-intensive and takes about 1 hour for each pair of images. Other aspects of the dynamics of protrusion and retraction can be measured by much simpler methods and, for this first analysis of the database, we simply take the areas of protrusion and retraction over a fixed time interval (Dunn, 1980; Dunn and Brown, 1987) and the mass of material contained in these areas. The analysis is restricted to freely moving, isolated cells and is intended to examine the cause/effect relationships between cell mass, spread area, protrusion and retraction during all phases of cell movement. Although protrusion and retraction areas are easily defined only for cells growing on plane smooth surfaces, they are closely related to the rates of fundamental motile processes that are assumed also to occur in vivo such as adhesion, de-adhesion, contraction and disassembly, transport and assembly of cytoskeletal components. Chen (1981) has presented evidence that even the violent retraction that follows the detachment of a fibroblast's tail involves an active contraction as well as a passive elastic recoil. Phase-stepping microinterferometry offers a unique insight into the dynamics of these processes, since it greatly facilitates the measurement of protrusion and retraction areas, as well as their masses, and allowed us to make many thousands of measurements for this study. Accurate information on the quantity and movement of non-aqueous material within living cells is not available by other methods and the automatic processing of images obtained by conventional microscopy has not yet advanced to the stage where even cell outlines can be recognised reliably.

MATERIALS AND METHODS

Cell culture

Hearts were removed from 7-day or 8-day chick embryos and washed in Hanks' saline. The atria were removed with a pair of cataract knives and the pericardia were carefully separated from the ventri-

cles with forceps. The ventricles were then placed in a drop of Hanks' saline and cut into small explants. Hanging drop cultures each consisted of two explants placed in a drop of medium on a 22 mm × 22 mm no. 2 cover glass, which was then sealed onto a cavity slide using a mixture of equal parts of beeswax, soft yellow paraffin and paraffin wax. The medium was Medium 199 with Hanks' salts (Flow) supplemented with 10% heat-inactivated foetal bovine serum (Gibco), 100 i.u. ml^{-1} penicillin and 100 μg ml^{-1} streptomycin (Gibco) and 1 mM glutamine (Flow). After incubation at 37°C for 24 hours, the explants were gently removed with forceps and the cell outgrowths carefully washed twice in the medium. After another day of incubation, each cover glass was mounted onto a Helber Bacteria Counting Chamber (Z3 special unruled, Weber Scientific International Ltd, Teddington, UK) for interference microscopy, leaving a small bubble of air trapped in the medium to ensure efficient buffering.

Phase-stepping interference microscopy and image recording

Culture temperature was maintained at 37°C by carrying out the interference microscopy in a temperature-controlled warm room. The recording field measured 485.2 μm × 342.4 μm using the 20× twin objective of the Horn type Transmitted-Light Interference Microscope (Leitz, Wetzlar, Germany) coupled to a TM-765 monochrome CCD camera (Pulnix Europe Ltd., Basingstoke, UK) of 756 × 581 pixels with the gamma set to 1.0 and the AGC disabled. Phase-stepping permits the relatively unstable Horn double-beam interference microscope to be used for long-term, time-lapse recording with the advantage that individual cells do not give displaced secondary images as with other transmission interference microscopes. The procedure is to acquire rapidly three or four digital images while adjusting the optical path of the microscope's reference beam in quarter wavelength steps using a stepper motor controlled by the host computer (Dunn and Zicha, 1994). Phase-stepping gives a map of the true retardation introduced by the cells, regardless of any variation in illumination or contrast across the microscope field, and the four-image method used here further compensates for second order nonlinearity of the camera's transfer function.

Each of the four digital images consisted of eight camera frames acquired at video rate, redigitised to 768 × 512 pixels × 256 grey levels, and then averaged using a DT2867 frame grabber and processor board (Data Translation, Wokingham, UK). The four images were then transferred to the host computer and the phase-stepped image of the retardation, ϕ, introduced by the cells was calculated on a pixel-by-pixel basis from the four intensities corresponding to each pixel location using the formula:

$$\tan(\phi) = \frac{I_4 - I_2}{I_1 - I_3}.$$

The total exposure time was 2.4 seconds per phase-stepped image and an automatic shutter prevented unecessary illumination of the cells between exposures. These images were recorded at 2-minute intervals over periods of 24 hours from three cultures of 7-day and three cultures of 8-day primary chick heart fibroblasts. The range of accurate measurement of retardation is one wavelength, which, for the green light used ($\lambda = 546$ nm), corresponds to 3 pg μm^{-2} of areal dry mass density. The fibroblasts in this study rarely exceeded a dry mass density of 2 pg μm^{-2}, even when rounded during division.
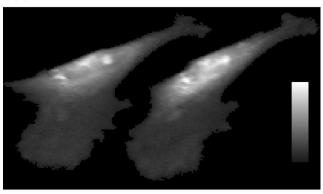
Image sequences were then processed to compensate for any drift in the microscope settings and to remove any residual distortion of the reference wavefront introduced by the microscope optics. The basis of this compensation is that the cell-free regions of the image (which must always be present to act as a reference) have a uniform dry mass density of zero (see Dunn and Zicha, 1994, for details). Each processed image sequence was finally compressed using run-length coding for the background grey level and archived on a rewritable optical disk.

Preliminary data analysis

Preliminary analysis of the data began by computing total dry mass, spread area and {x,y} coordinates of the mass centroid for each cell or cell cluster within each phase-stepped image of a sequence. These measures were obtained by numerical integration of the dry mass distribution of each object (Brown and Dunn, 1989). This process was entirely automatic. The images were next displayed on a computer as a movie sequence while the operator identified each cell by keeping a cursor positioned within its boundary using a mouse control. When all visible cells in the culture had been treated in this manner, the computer was able to construct a table linking the objects that it had detected and measured to the cells identified and named by the operator. The final result of this stage was a list of all the cells, cell clusters and cell fragments in all the frames together with their time, mass, area and centroid data. The analysis of these data was carried out in *Mathematica* (Wolfram Research Inc., Champaign, Illinois, USA). After rejecting data from cell clusters and fragments, the remaining broken sequences of data consisted of 13,395 sets of measurements from a total of 170 isolated fibroblasts extracted from the six recordings.

Further information about each cell was either computed in *Mathematica* or computed from the image sequence using a special request procedure. Fig. 1A shows the distribution of dry mass in a single fibroblast taken from two successive frames of a recording. The dif-

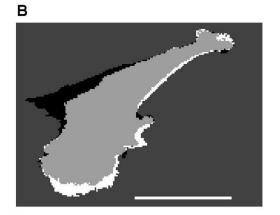### 1 A

B

Fig. 1. (A) A composite image of two dry mass distributions from a single chick heart fibroblast taken from portions of two consecutive recorded frames. The grey scale in this figure covers a range of dry mass density from 0.01 (darkest grey) to 0.6 (white) pg μm^{-2}, which is 1/5 of the full measurement range. (B) The two outlines of the cell are shown superimposed in their correct relative positions with the 2-minute retraction area shown in black and the 2-minute protrusion area shown in white. Bar, 40 μm.

ference between the total mass of the two distributions, multiplied by 30, gave an estimate of the hourly growth rate, and dividing this by the mean of the two masses gave the relative hourly growth rate. The vector difference of the mass centroid positions gave the 2-minute displacement vector - a measure of cell translocation. In Fig. 1B, the two outlines of the cell are shown superimposed in their correct relative positions with the 2-minute retraction area shown in black and the 2-minute protrusion area shown in white (Dunn and Brown, 1987). The retraction mass and protrusion mass were obtained by integrating the dry mass density within the corresponding areas. These image-differencing methods yielded 12,596 sets of data from 799 continuous sequences. Intracellular details are not clearly visible in Fig. 1 since we have sacrificed high spatial and temporal resolutions in this study in order to obtain long-term data from as many cells as is practicable.

RESULTS

Relation of spreading to mass

Fig. 2 shows the dry mass of the 7-day primary cells plotted as trajectories against time. It is clear from these trajectories that the great majority of cells were increasing in mass throughout the 24 hour period with no obvious diminution of this growth rate. The mean and s.e.m. of the hourly growth rate is 4.47±0.51 pg h^{-1} for the 7-day cells and 4.16±0.69 pg h^{-1} for the 8-day cells. These were not significantly different in a two-tailed *t*-test. The relative growth rates are 0.0208±0.0024 h^{-1} and 0.0209±0.0035 h^{-1}, respectively, obviously not significantly different. The respective doubling times for mass, calculated by dividing $\log_e 2$ by the relative growth rates, are 33.40 hours and 33.14 hours. This doubling time is probably not an accurate estimate of the cell cycle period, since cell cycling is unlikely to have reached a steady state in these primary cultures.
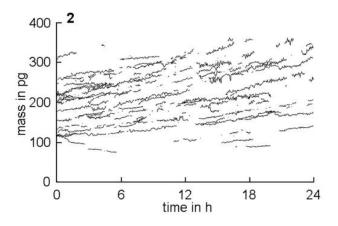

Fig. 2. Trajectories of dry mass in pg versus time in hours for the 7-day cultures. Breaks in the individual trajectories correspond chiefly to periods when the cells are in contact with others, though they may also result from cells leaving the field of view or dividing. The excessive noise associated with some of these growth trajectories is due to measurement errors caused by rapid cell movement. We have now improved this for growth studies by using continuous phase-shifting over eight video frames to achieve an exposure time of 0.32 second instead of the 2.4 second exposures of this study. Larger spikes and dips on the traces are caused by cells colliding with debris or leaving small fragments attached to the substratum.
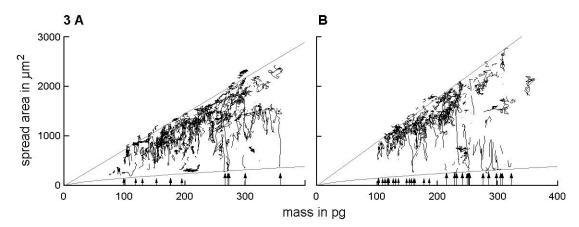
Fig. 3. Trajectories of spread area in μm² versus dry mass in pg for the 7-day cells (A) and for the 8-day cells (B). The straight inclined line in each plot indicates the approximate upper limit on spreading per unit mass, which is 7.2 μm² pg⁻¹ (A) and 8.8 μm² pg⁻¹ (B). The lower curve in each plot is the equatorial, cross-sectional area of a sphere of density 0.07 pg μm⁻³ plotted as a function of its mass. Long arrows and short arrows indicate the masses of cells measured within 1 hour before or after cytokinesis, respectively.

Fig. 3A shows trajectories of the 7-day cells and Fig. 3B of the 8-day cells plotted on the plane of spread area versus total dry mass. Arrows on each plot indicate the masses of mother cells (long arrows) and daughter cells (short arrows) for cases where it was possible to measure isolated cells within one hour of division. The almost vertical trajectories in the region of 280 pg in the figures represent cells rounding up and almost all coincide with the arrows marking mother cells. Trajectories for the respreading of daughters, in the region of 140 pg, are generally incomplete, since daughters tend to remain in contact during early stages of spreading. In ten cases it was possible to compare the masses of the two daughters within 0.5 hour of the moment of their separation and these can show a surprisingly high disparity: the ratio of heaviest to lightest was greater than 1.2 in four cases with a maximum of 1.35. Since the masses of mothers and daughters are reasonably well segregated, the plots are pictures of the typical spreading activity throughout the cell cycle.

The spreading activity is confined to a roughly triangular region in each plot with a particularly sharp and linear upper boundary indicated by the straight line extending to the origin. Thus the maximum area to which a cell can spread appears to be strictly dictated by its mass, although this limit seems to be different for the 7-day and 8-day cells. The 7-day cells spread up to a limit of 7.2 μm² pg⁻¹ and 8-day cells to 8.8 μm² pg⁻¹ as indicated by the inclined lines. Except for the vertical trajectories associated with division, the lower part of each triangular region is almost devoid of cellular activity and it therefore seems that, during interphase, these cells rarely reduced their area to less than about half of the maximal area. The absolute lower limit on spread area is defined by the rounded cells and, assuming that these are truly spherical, they have a dry mass density close to 0.07 pg μm⁻³ as indicated by the theoretical curve for spheres of this density in the lower part of each plot. With the further assumption that all the cells have the same density, this allows us to calculate that the 7-day cells did not spread more thinly than a mean cellular thickness of 1.98 μm and the 8-day cells not more thinly than 1.62 μm.

It is unlikely that cellular thickness is the factor limiting spreading, however, since thickness varies widely in the different regions of a cell. A more plausible explanation is that some substance is present in direct proportion to dry mass, possibly an adhesion molecule or cell surface component, that permits the cell to spread to a corresponding maximal area. Preliminary observations of detached cellular fragments suggest that this is also unlikely to be the full explanation, since these fragments usually exceeded the limiting area-to-mass ratio at the moment of detachment but collapsed to within the limit over the next few minutes. We favour explanations in which the area of spreading is dynamically regulated.

A possible dynamic model of mass-limited spreading is that some molecule essential for adhesion is produced at a rate proportional to the cell's mass and is lost at a rate proportional to the cell's area. Assuming that the area of spreading is directly proportional to the number of adhesion molecules present, the rate of change in area is given by the difference between the rate of production and the rate of loss which results in a first-order ordinary differential equation:

$$\frac{\mathrm{d}A(t)}{\mathrm{d}t} = k_1 M - k_2 A(t) \, ,$$

where $A(t)$ is area as a function of time, M is mass (assumed to be a parameter) and k_1 and k_2 are rate constants. If $A(0)$ is set to zero, this equation has the solution:

$$A(t) = \frac{k_1 M}{k_2} \, (1 - e^{-k_2 t}) \, .$$

As t increases, the second term in the final brackets tends to disappear and so the model cell spreads until its area is equal to $k_1 M/k_2$. When it reaches this limiting area, the rate of production of the molecule equals its rate of loss.

Relation of protrusion to retraction

For the real chick fibroblasts, the rate of change in area can also be viewed as the difference between two rates, in this case the rate of protrusion and the rate of retraction, and we were curious as to whether these measurable rates might bear some relation to the theoretical rates of the differential equation. The rates were measured as 2-minute protrusion and retraction
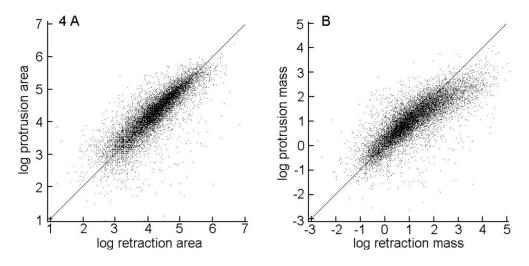
Fig. 4. In each of these scatter plots, the 12,596 data pairs are represented by 12,596 points. Taking logarithms yields an approximately normal bi-variate distribution which would otherwise be highly skewed. (A) $\log_e$ (protrusion area in µm²) versus $\log_e$ (retraction area in µm²). (B) $\log_e$ (protrusion mass in pg) versus $\log_e$ (retraction mass in pg).

areas as illustrated in Fig. 1B, and Fig. 4A shows the relationship between the simultaneous protrusion and retraction areas on a log/log scatter plot. It is clear that there is a high correlation between the rates of protrusion and retraction and also a high symmetry about the diagonal line which represents equal rates. In fact the correlation coefficient between the logarithms of protrusion and retraction areas is 0.865 but these are the pooled data for all cells and a high correlation could arise if protrusion and retraction tend to be similar within cells but different between cells, possibly because of their different masses. Time-series analysis avoids this problem by calculating the dynamic correlation within each continuous sequence of data. It is then possible to pool the correlation coefficients, after weighting them suitably, and the legend of Fig. 5 describes how this was done for the 799 continuous sequences of data. In the cross-correlation of Fig. 5A, there is still a high correlation of 0.601 between the logarithms of simultaneous values of protrusion and retraction area. The correlations fall off rapidly, however, if there is a time lag between the protrusion and retraction values and they almost reach zero for lags of greater than 20 minutes. The autocorrelations of Fig. 5B,C

and D show that both protrusion and retraction areas fluctuate rapidly, retraction slightly more so than protrusion, whereas the total spread area of the cell fluctuates far less rapidly than either. We conclude that protrusion and retraction areas are closely interlinked so that their simultaneous values tend to be similar. This tends to keep the spread area of the cell constant and suggests that spreading is kept under close control over short time intervals. Closer examination of Fig. 5A reveals that protrusion is still highly correlated with the retraction of 2 minutes earlier ($r = 0.505$) but less correlated with the retraction of 2 minutes later ($r = 0.419$). A similar pattern is observed at longer lags. This is evidence that the fluctuations in retraction slightly precede the fluctuations in protrusion and may actually cause them.

One possible mechanism that could account for the close dynamic link between protrusion and retraction is that retraction involves disassembly of cellular material, which is then rapidly transported to other parts of the cell periphery to be reassembled into protrusive structures. A short delay incurred by the transport, of the order of less than one minute, would account for the slight lag between the fluctuations in retraction
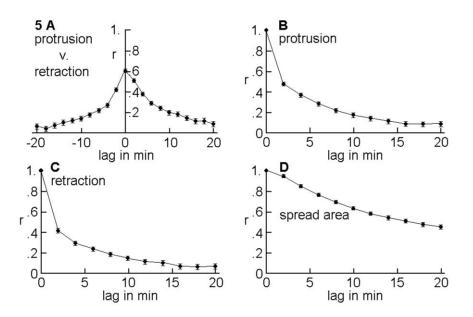

Fig. 5. (A) The pooled cross-correlation between $\log_e$(protrusion area) and $\log_e$(retraction area) at each different lag time is obtained by taking the correlation for each continuous sequence of data and calculating the weighted mean for all sequences after applying Fisher's z transformation and correcting for Fisher's bias (see Snedecor and Cochran, 1967, pp. 186-188). The 99% confidence limits on each correlation are calculated using Fisher's z transformation and hence are asymmetrical. The autocorrelations of $\log_e$(protrusion area) at different lag times (B), the autocorrelations of $\log_e$(retraction area) at different lag times (C) and the autocorrelations of $\log_e$(spread area) at different lag times were all calculated by the same method as the cross correlations.

and protrusion. Fig. 4B is a log/log plot comparing the mass of cellular material withdrawn from the retraction area with the mass of material that occupies the newly protruded area. It can be seen that, when the retraction rate is high, the amount of material protruded is considerably less than the amount retracted. In comparison with Fig. 4A, the masses of simultaneous protrusion and retraction are obviously less closely related than their areas. This suggests that the matching of protrusion and retraction areas is the primary mechanism and the masses become correlated, but less so, because the amount of material occupying the retraction and protrusion sites is roughly proportional to their areas. The matching of areas could still result from a rapid transport mechanism, provided that some of the material transported was involved in cell/subtratum interaction. For example, if adhesion molecules were reused for protrusion soon after they became available from retraction sites, then the area of protrusion would be expected to be closely matched to the area of retraction of a short time earlier.

Relation of protrusion and retraction to spreading

To recap, it seems that, in the short term, spreading is buffered against the rapid fluctuations in protrusion and retraction and, in the long term, spreading is limited in direct proportion to the mass of the cell. We have suggested that both controls might be mediated by the supply of some molecule essential for spreading. An interesting possibility is that a limited supply of the same molecule might account for both phenomena. The relationship of area to mass could be achieved, as before, by the rate of production of the molecules being proportional to the mass of the cell and the rate of loss proportional to the cell's area. Adhesion molecules are most likely to be lost or destroyed during their detachment, as the cell pulls away from the substratum, and their rate of loss might therefore be expected to be closely related to the area of retraction. Their rate of loss would also be related to the cell's spread area provided that the area of retraction were closely related to the cell's area. The high correlation between protrusion and retraction areas could be achieved if the remaining molecules released by retraction were rapidly recycled into the protrusion sites. Thus the protrusion area would also be expected to be related to the cell's spread area. We tested these ideas by examining the relationship of retraction and protrusion to the cell's spread area.

The relationship between retraction area and spread area for the chick fibroblasts is shown in Fig. 6A and it can be seen that, as expected, the retraction values fluctuate wildly but tend to increase with increasing spread area. The relationship between protrusion area and spread area, shown in Fig. 6B, is very similar, which is also to be expected from the high correlation between simultaneous values of retraction and protrusion. By comparing the standard deviations of protrusion and retraction in the two figures, it can again be seen that the fluctuations in retraction are slightly greater than those in protrusion. The most unexpected feature of the plots is the sharp lower limit on both retraction and protrusion values. The small clump of points on the extreme lower left of each plot represents the periods during which cells are rounded for division and consequently show little motile activity. During the rest of the time, the 170 cells all show incessant activity and it is remarkable that neither the protrusion area nor the retraction area ever falls much below about 1/40 of the spread area as indicated by the inclined lines in each plot. These lower boundaries are quite sharp and similar plots against the masses instead of the areas of the cells (not shown) have much less well defined lower boundaries. This suggests that the rates of retraction and protrusion are fundamentally related to the spread area of the cell. It is as if 2.5% of the spread area of the cell must detach from the substratum during each 2-minute interval and that this inevitable detachment can sporadically trigger much larger areas of detachment.

Relation of protrusion and retraction to translocation

Protrusion and retraction not only determine the rate of change in area of the cell but also its rate of translocation. In this case it is the relative distribution of the sites of protrusion and retraction that is important. In a fully polarised cell, in which protrusion takes place at the opposite end of the cell from retraction, the observed minimal rates of protrusion and retraction are sufficient to completely displace the cell into new territory within 80 minutes. Chick fibroblasts typically move their own length in an hour (Abercrombie, 1980) and so these minimal rates of protrusion and retraction are almost capable of accounting for the typical translocation activity. Since protrusion and retraction rates are generally much greater than this minimal level, it is clear that they are not usually fully polarised. This is confirmed in Fig. 7, which shows retraction area (A) and protrusion area (B) for non-rounded cells (cell area > 1000 μm^2) plotted against the net displacement of the
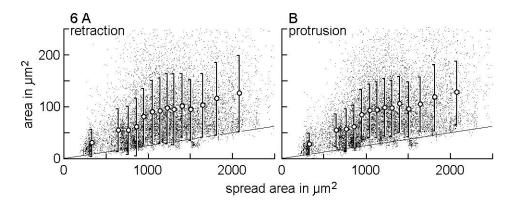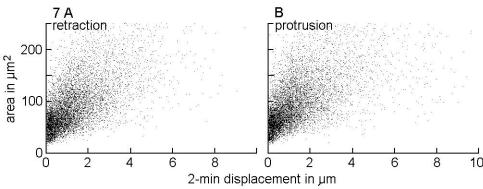

Fig. 6. In each of these scatter plots, the 12,596 data pairs are represented by 12,596 points. The straight inclined line in each plot indicates 2.5% of the spread area. Superimposed on each plot is the mean and standard deviation of the respective retraction or protrusion area at 14 values of mean spread area. These were obtained by sectioning the data into 14 equal-sized subsamples after sorting them in order of ascending spread area. (A) Retraction area in μm^2 versus spread area in μm^2. (B) Protrusion area in μm^2 versus spread area in μm^2.

Fig. 7. In each of these scatter plots, only the 7,934 data pairs corresponding to spread areas of greater than 1,000 μm^2 are shown. Retraction area in μm^2 (A) and protrusion area in μm^2 (B) versus magnitude of 2-minute displacement vector in μm.
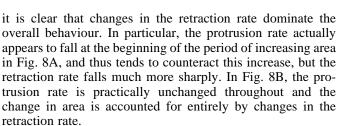
cell centroid. Evidently, both retraction and protrusion continue incessantly in non-rounded cells, even when there is no net translocation of the cell, and so cell translocation cannot account for the minimal levels of protrusion and retraction. We conclude that protrusion and retraction are much more constant activities than translocation and that it is a loss of polarity rather than a cessation of protrusion/retraction activity that brings the cells to a halt. In other words, stationary cells are still actively changing shape on the spot.

Behaviour of protrusion and retraction during changes in spread area

Despite the generally close match between simultaneous protrusion and retraction, it is clear from Fig. 3 that the areas of the cells do change considerably even during interphase. When the area of a cell increases, the protrusion area must exceed the retraction area and vice versa for falls in area. Thus the diagonal line in Fig. 4A separates increases in area from decreases. Distinct differences in the dynamic behaviour of protrusion and retraction emerged when we analysed their rates during such changes in area. We did this by selecting all sequences of data that match specific patterns. We chose first to find all sequences of data of length 32 minutes in which a central subsequence of length 10 minutes showed a continuous rise in area, with no other constraints. 517 such sequences were found and changes in the mean spread area, mean protrusion area and mean retraction area during these sequences are shown in Fig. 8A. Continuous falls in area tend to be steeper and of shorter duration and so we specified a central subsequence of continuously falling area for 8 minutes. This choice gives a comparable absolute change in area as shown in the plot for 238 falling sequences in Fig. 8B. In both plots,

it is clear that changes in the retraction rate dominate the overall behaviour. In particular, the protrusion rate actually appears to fall at the beginning of the period of increasing area in Fig. 8A, and thus tends to counteract this increase, but the retraction rate falls much more sharply. In Fig. 8B, the protrusion rate is practically unchanged throughout and the change in area is accounted for entirely by changes in the retraction rate.

It seems almost paradoxical that protrusion and retraction should appear to behave independently during sustained changes in area when they show a high mutual dependency at other times. In order to satisfy ourselves that this and other aspects of the apparently complex behaviour could result from a relatively simple mechanism based on a limited supply of adhesion molecules, we attempted to simulate the behaviour using a computer model.

A stochastic model of fibroblast spreading

Unlike the first model, which is deterministic, the new model is stochastic and uses pseudo-random number generators to imitate the fluctuations in cell behaviour. Since the cross-correlation of Fig. 5A suggests that the fluctuations in retraction slightly precede the fluctuations in protrusion, it likely that the fluctuations originate in the retraction process. The dynamic analysis of continuous changes in the cell's area also indicates that these are not caused by changes in the rate of protrusion, but in the rate of retraction. We therefore place the stochastic generator at the site of retraction in the model. It also makes sense from the biological point of view that fluctuations originate during the retraction process, since a moving fibroblast is under tension and the detachment of small adhesion sites can sporadically lead to rapid and extensive retractions as other
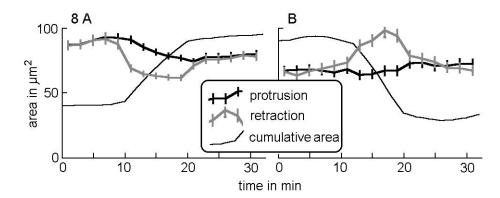

Fig. 8. Plots of mean protrusion area in μm^2, mean retraction area in μm^2 and cumulative changes in area in $2 \times \mu m^2$ in selected 32-minute sequences of data versus time in minutes from the start of each sequence. Protrusion area and retraction area have error bars indicating the s.e.m. and the cumulative area is given an arbitrary starting value of 80 μm^2 (A) and 180 μm^2 (B) at the beginning of each sequence. (A) 517 sequences in which area was rising continuously between 10 and 20 minutes. (B) 238 sequences in which area was falling continuously between 12 and 20 minutes.
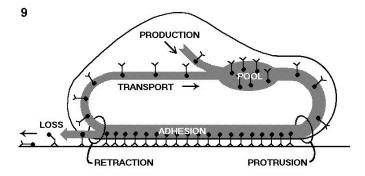
9

Fig. 9. The scheme of the stochastic model of retraction, protrusion and spreading behaviour. The number of adhesion molecules in the soleplate of the cell is proportional to the cell's spread area. The remainder of the molecules are held in the internal pool (although molecules are also shown being transported in the diagram). New molecules are added to the pool at a rate proportional to the cell mass. Protrusion withdraws molecules from the pool in proportion to the pool's current size and adds them to the soleplate. Retraction removes molecules from the soleplate at random with a mean rate proportional to the size of the soleplate. A random proportion of the molecules freed by retraction is lost and the rest are added to the pool.

adhesion sites yield under the increased tension transferred to them.

The scheme of the new model is illustrated in Fig. 9. For simplicity, it is assumed that one of the hypothetical adhesion molecules supports one square micrometre of spread area. The cell's area at any time is therefore numerically equal to the number of adhesion molecules in the soleplate of the cell. The remainder of the adhesion molecules are held in the internal pool shown in the diagram. New molecules are added to this pool at a rate proportional to the cell mass. Mass increases exponentially at a rate chosen to match the chick fibroblasts' relative growth rate. Protrusion transfers molecules from the pool to the soleplate at a rate proportional to the size of the pool. Retraction removes molecules from the soleplate at random with a mean rate proportional to the size of the soleplate. A random proportion of the molecules freed by retraction is lost and the rest are recycled into the pool. This satisfies the requirement that the mean rate of loss of the adhesion molecules is proportional to the spread area of the cell. We must emphasise that the molecular details of the model are not intended to be realistic, and it is particularly unrealistic to assume that the soleplate is uniformly adherent, but our intention is to model processes and not structures.

The kernel of the model is the stochastic generator which determines the fluctuations in retraction. While keeping this as simple as possible, we have tried to give it some of the characteristics of the real retraction process. An autoregressive term simulates the observed autocorrelation for fibroblast retraction and the random number generator is designed to give a very skewed distribution, with occasional values many times greater than the mean, similar to the observed distribution of retractions. Also, we have included a constant term in the random number generator which ensures that retraction never falls below a certain percentage of the area. We have no explanation of this observed fact and simply incorporate it into the model. The random loss of molecules freed by retraction is

simulated by a simple uniform random number generator. All the rest of the model is a deterministic consequence of this stochastic kernel. Parameters of the model were adjusted to mimic the autocorrelation and cross-correlation structure of the real data at lags of 0 and 2 minutes. Details of the algorithm and the computer code for the model are given in the Appendix.

We present the results of simulating 200 sequences on the model. Each sequence has 50 sampling times representing 100 minutes duration. For each sequence, the starting values of mass and area are the same as the finishing values of the previous sequence except in the case of the first sequence or in cases in which the mass value has become unrealistically high. These exceptional cases were initiated with a new mass value chosen at random in the range 100-200 and a new area value chosen at random to be less than eight times the mass. In effect, these newly initiated sequences represent new cells and so we are simulating several cells with several sequences taken from each cell; which is much like the real data except that the simulated sequences are of uniform length.

Fig. 10A shows the area versus mass plot for the simulated data. It compares favourably with Fig. 3A and B although, not surprisingly, the simulated cells appear to be more uniform in their spreading characteristics than the real cells. The diagonal line indicates 7.2 μm^2 pg^{-1}, which is the mass-related spreading limit for the 7-day fibroblasts. Since the simulated cells are initialised with areas often well below this limit, vertical trajectories in the left-hand part of Fig. 10A imitate the spreading of daughter cells. However, the rounding up of mother cells is not represented. The simulated cells will round up quite quickly if the production of the hypothetical adhesion molecules is switched off but we did not wish to assume that this corresponds to the real mechanism for rounding up. Fig. 10B shows the scatter plot of log(protrusion area) versus log(retraction area) for the simulated data. Again the result is quite similar to the real data of Fig. 4A. Also, scatter plots of simulated data for retraction area and protrusion area plotted against spread area, shown in Fig. 10C and D, respectively, have much similarity with the real data shown in Fig. 6A and B. In this case the protrusion values do show a lower variance than the retraction values, as with the real data, though this effect seems to be exaggerated in the simulated data. A major test of the model is whether its dynamic behaviour during sustained increases and decreases in area is similar to that of the real data. Fig. 10E and F shows that the simulated data behave remarkably like the real data of Fig. 8. The data for rising area are particularly alike and, although the simulated protrusion does not remain as constant as the real protrusion during falls in area, the dominance of retraction is evident.

We conclude that the major features of the spreading activity of the chick fibroblasts can be reproduced in a simple model. Further refinements of the model may well improve its correspondence with the real data but we think that a more complex model may be less convincing, since increasing the number of parameters increases the model's ability to fit any data.

DISCUSSION

Our finding that the spread area of the fibroblasts is limited in direct proportion to their dry mass was unexpected. We expected, of course, that the area would tend to increase with
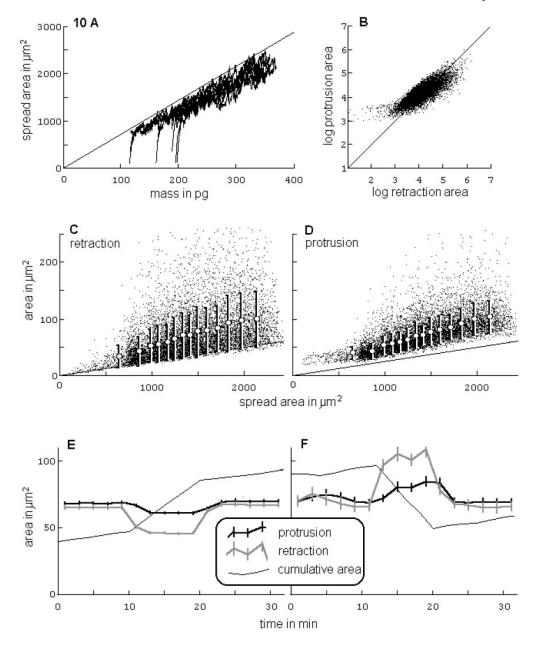
Fig. 10. The results of simulating 200 sequences on the model. (A) Spread area versus mass plot for the simulated data. The inclined line indicates 7.2 μm^2 pg^{-1} which is the mass-related spreading limit for the 7-day fibroblasts. (B) Scatter plot of $\log_e$(protrusion area) versus $\log_e$(retraction area) for the simulated data. Scatter plots of simulated data for retraction area (C) and protrusion area (D) plotted against spread area. See legend to Fig. 6 for details. Plots of mean protrusion area, mean retraction area and cumulative changes in area in selected 32-minute sequences of rising spread area (E) and falling spread area (F) for the simulated data. See Fig. 8 for details.

increasing mass but, if larger cells behaved like scaled up versions of smaller ones, then the area would be proportional to mass raised to the power of 2/3 and this is clearly not the case. On the other hand, if the lamellar region of a cell could not spread more thinly than a certain limiting thickness, then the maximal area of this region would be expected to be proportional to its mass. But this is equivalent to saying that the areal mass density of the lamellar regions of fully spread cells would be constant and uniform, and we found no evidence for this. Furthermore, the lamellar region contains only a fraction of the cell's mass whereas restrictions on thickness would have to apply to the whole cell in order to account for the cell's maximal area being directly proportional to its mass. These considerations led us to suspect that spread area might be actively controlled in relation to cell mass rather than just an incidental consequence of the cell's geometry. Such control might be important because it is conceivable that the rates of

many interactions of the cell, with both the fluid and solid phases of its environment, are proportional to spread area whereas many metabolic rates are proportional to mass. Keeping these rates in balance would thus depend on maintaining the area-to-mass ratio.

A cell could limit its spread area in relation to its mass by restricting the quantity of some material essential for spreading. This might be a molecule directly involved in adhesion or it could equally well be an essential component of the cell surface or sub-surface cortex, since the total surface area of a maximally spread fibroblast is probably little more than twice its spread area. This static arrangement leaves little scope for active control, however, and there is some evidence that active control occurs. The peripheral region of a cell is usually spread much more thinly than the central region and so, if we consider the area-to-mass ratio measured separately for each region, that for the peripheral region is much greater.

If a fragment of a cell's periphery becomes detached from the main cell body without rounding up, therefore, it will probably exceed the limiting area-to-mass ratio for whole cells. Our occasional observations of such detachments confirm that the fragments can exceed this limit, at the moment of detachment, but then they decrease their area to within the limit over the next 20 to 30 minutes. These fragments usually continue to translocate for several hours but their area never again exceeds the limit. We have suggested that mass limited spreading might be explained if the hypothetical adhesion molecules were continuously produced at a rate proportional to mass and lost at a rate proportional to area. This would accord with the behaviour of fragments, since, after detachment, the rate of loss from a fragment would exceed the rate of production, thus reducing the area until the rate of loss matched the rate of production.

It appears that the fibroblasts also have a mechanism for minimising short term fluctuations in spread area. As with the tail detachment experiments described in the Introduction, the data presented here suggest a causal relationship between retraction and protrusion. The tail detachment experiments showed that a sudden large retraction leads, after a short delay, to a wave of increased protrusion. At other times, however, it is possible that the cause/effect relationship becomes reversed: that a large spontaneous protrusion could lead to an increased retraction as suggested by Weiss and Garber (1952). But the cross-correlation that we have found between protrusion and retraction areas suggests that fluctuations in retraction always lead those in protrusion; retraction is always the cause and protrusion the effect. Here the time resolution is not high enough to resolve the lag between retraction and protrusion but the asymmetry of the cross-correlations suggests that protrusion lags about 30 seconds behind retraction, which is consistent with the tail detachment observations. The higher variance and lower autocorrelations of retraction area as opposed to protrusion area reinforce this view that the origin of the fluctuations lies in the retraction process. We conclude tentatively that the fluctuations in retraction are spontaneous and beyond the cell's control; they would lead to large flutuations in the cell's spread area if they were not rapidly compensated by corresponding changes in the rate of protrusion.

We have suggested that the cell's mechanism of compensating for fluctuations in retraction might be merely to restrict the supply of some molecule so that large protrusions can only occur when the pool of molecules made available by retraction is large. Of course, it would be very surprising if new protrusions did not utilise material released by retraction and it is clear from the observations of Brown and Dunn (1989) that a large quantity of material is rapidly transported through the cell following tail detachment. However, we have shown here that the bulk of material transported into the newly protruded area is usually not sufficient to compensate for the material withdrawn from the retraction area when the retraction is large. The fact that protrusion area does tend to compensate fully for retraction area, even when retraction is large, indicates that the supply of some molecule essential for spreading, rather than the bulk flow of material, is responsible for determining the protrusion area. Although we have here suggested the most direct possibility - that it is a molecule associated with cell attachment - we have no evidence to dispute the conclusion of Chen (1979) that '...retraction of a portion of a fibroblast may

make cell surface (and associated cytoplasmic material) available for renewed spreading elsewhere...'

Our conclusions that the mass-limited spreading and the relationship between protrusion and retraction might both be mediated by a limited supply of a cell adhesion molecule led us to formulate a model in which the same molecule accounts for both phenomena. Since the mass-limited spreading requires that the molecule is lost at a rate proportional to spread area, and since it seemed most likely to us that the loss might occur during retraction, we expected to see some special relationship between retraction area and spread area. The relationship we found was surprising, however, and showed that retraction never becomes quiescent in non-rounded cells. We have no explanation of why at least 2.5% of the cell's area always retracts during each two minutes. A limited lifetime of adhesive structures would ensure a minimum level of retraction in the long term but then we might expect no retraction in the interval following a massive retraction which had removed all the adhesions near to the end of their life. Protrusion also shows a minimum level of 2.5% of the cell's area but this follows from the close relationship between protrusion and retraction, and requires no separate explanation. Whatever its cause, the lower limit on retraction demonstrates that there is a special relationship between retraction and area, rather than just between retraction and cell size, since the limit is not clearly demarcated when retraction is plotted against cell mass. The incessant activity of protrusion and retraction reveals that the locomotory 'engine' of the spread cell is running all the time but it only results in efficient locomotion when the sites of protrusion and retraction are polarised.

The model demonstrates that the mass-limited spreading behaviour of the cells and the relationship between protrusion and retraction could be different aspects of a single simple mechanism for controlling spreading. The origin of all fluctuations in the model lies in the retraction process and a test of whether this is also true for real fibroblasts is to compare their dynamic behaviour with that of the model. Unlike the tail detachment experiments, here cell behaviour is not experimentally manipulated and so we cannot tell directly which changes in cell area are spontaneous and which might be the results of some regulatory mechanism; both processes are occurring simultaneously and the changes will be superimposed. Changes in spread area occur when the simultaneous rates of protrusion and retraction do not match and, in the case of the model, these occur because protrusion does not compensate adequately for a changed rate of retraction. The dynamic behaviour of the model is too complicated for us to analyse rigorously but it is perhaps not surprising that sustained changes in area are accompanied by a changed rate of retraction without a compensatory change in the rate of protrusion. The fact that the real fibroblasts show similar dynamic characteristics is evidence for a similar mechanism: that the spontaneous fluctuations have their origin in the retraction process and that protrusion is a compensatory process. This conclusion is reinforced by the earlier evidence that the fluctuations in retraction are the cause, rather than the effect, of the fluctuations in protrusion.

REFERENCES

Abercrombie, M. (1980). The crawling movement of metazoan cells. *Proc. Roy. Soc. B* **207**, 129-147.

Bereiter-Hahn, J. (1985). Computer assisted microscope interferometry by image analysis of living cells. In *Advances in Microscopy. Progress in Clinical and Biological Research*, vol. 196 (ed. R. R. Cowden and F. W. Harrison), pp. 27-44. Alan R. Liss, New York.

Brown, A. F. and Dunn, G. A. (1989). Microinterferometry of the movement of dry matter in fibroblasts. *J. Cell Sci.* **92**, 379-389.

Chen, W.-T. (1979). Induction of spreading during fibroblast movement. *J. Cell Biol.* **81**, 684-691.

Chen, W.-T. (1981). Mechanism of retraction of the trailing edge during fibroblast movement. *J. Cell Biol.* **90**, 187-200.

Davies, H. G. and Wilkins, M. H. F. (1952). Interference microscopy and mass determination. *Nature* **169**, 541.

Dunn, G. A. (1980). Mechanisms of fibroblast locomotion. In *Cell Adhesion and Motility*, 3rd BSCB Symposium (ed. A. S. G. Curtis and J. D. Pitts), pp. 409-423. Cambridge University Press, Cambridge.

Dunn, G. A. and Brown, A. F. (1987). A unified approach to analysing cell motility. *J. Cell Sci. Suppl. 8*, 81-102.

Dunn, G. A. and Zicha, D. (1993). Phase-shifting interference microscopy applied to the analysis of cell behaviour. In *Cell Behaviour: Adhesion and Motility*, S.E.B. Symposium XLVII (ed. G. Jones, C. Wigley and R. Warn), pp. 91-106. The Company of Biologists Ltd, Cambridge.

Dunn, G. A. and Zicha, D. (1994). Using interference microscopy to study cell behaviour. In *Handbook of Cell Biology* (ed. J. E. Celis), pp. 25-33. Academic Press Inc., London, New York.

Snedecor, G. W. and Cochran, W. G. (1967). *Statistical Methods*, Sixth Edition. p. 186. Iowa State University Press, Ames, Iowa.

Weiss, P. and Garber, B. (1952). Shape and movement of mesenchyme cells as functions of the physical structure of the medium. Contributions to a quantitative morphology. *Proc. Nat. Acad. Sci. USA* **38**, 264-280.

Appendix

The code is written in *Mathematica*. After initialising the variables, the outer table is entered, which simulates the two-minute sampling rate and eventually generates 50 sequential values for mass, area, protrusion and retraction. Within this table, cell growth is first simulated by multiplying the current mass by 1.0007 to obtain each new table entry for mass. This approximates the relative growth rate of the fibroblasts. Next an inner table is entered which runs four times as fast as the sampling rate and generates four incremental values for protrusion and retraction. This allows fluctuations in protrusion to be delayed approximately 30 seconds behind fluctuations in retraction. For each new entry in this table, the protrusion increment consists of 60% of the adhesion molecules in the internal pool. Next the new retraction increment is composed of 60% of the previous retraction increment (this simulates the observed autocorrelation for fibroblast retraction) together with a random proportion of the current spread area determined by ranGenA. Finally, the pool is updated by withdrawing the molecules that were used for protrusion, adding a random proportion of the molecules freed by retraction (determined by ranGenB) and adding newly produced molecules in fixed proportion to the cell's current mass. Back in the outer table, the four incremental values for protrusion and retraction are summed to obtain the new entries for protrusion and retraction and the spread area of the cell is updated as the old value plus protrusion minus retraction.

```
(*CELL SPREADING MODEL*)

ranGenA[] := 0.002+0.2*Random[]*Random[]*Random[]*Random[]*Random[]*Random[];
ranGenB[] := Random[];

mass    =     150.0;                                    (*Initialise variables*)
area    =     600.0;
pool    =      10.0;
dRetr   =     0.01*area;

Table[                                                  (*begin outer table*)
       mass = 1.0007*mass;                              (*update cell mass*)
       {protrusion, retraction} = Apply[Plus,          (*accumulate 2-min protrusion & retraction*)
       Table[                                           (*begin inner table*)
              dProt  = 0.6*pool;                           (*30-s protrusion increment*)
              dRetr  = 0.6*dRetr+ranGenA[]*area;           (*30-s retraction increment*)
              pool   = pool-dProt+ranGenB[]*dRetr+0.04*mass;  (*update pool*)
              {dProt, dRetr},                              (*new inner table entry*)
       {dt, 4}]                                         (*inner table index*)
       ];
       area = area+protrusion-retraction;              (*update cell area*)
       {frame, mass, area, protrusion, retraction},     (*new outer table entry*)
{frame, 50}]                                            (*outer table index*)
```